PHYSICAL REVIEW A **107**, L061101 (2023)

Letter

# Cavity Jahn-Teller polaritons in molecules

Krishna R. Nandipati[*] and Oriol Vendrell[†]
*Theoretische Chemie, Physikalisch-Chemisches Institut, Universität Heidelberg, Im Neuenheimer Feld 229, 69120 Heidelberg, Germany*

(Received 7 November 2022; accepted 25 May 2023; published 9 June 2023)

Jahn-Teller (JT) polaritons emerge when the two perpendicular, normal-incidence electromagnetic modes of a Fabry-Perot cavity interact with JT active systems. These JT polaritons are characterized by a mixed $(+/-)$–circular electromagnetic polarization mediated by the molecular JT vibronic coupling of the material subsystem. Consequently, the exchange of photonic and vibronic angular momenta can be very efficient. Due to the photonic-vibronic coupling, the magnitude and direction of the cavity polarization varies for different eigenstates of the cavity-molecule system. This type of light-matter coupling results in polarization inverted states in the polaritonic system—states that can be reached resonantly with either right or left circularly polarized light but which are characterized by a cavity-photon polarization opposite to the external fields used to excite the system.

DOI: 10.1103/PhysRevA.107.L061101

*Introduction.* The formation of polaritons and identification of their light-matter composition are key to understanding cavity-controlled processes in molecules [1–14] and materials [15–17]. Polaritons with mixed electronic, vibrational, and photonic character promise a new handle to achieve cavity-controlled photophysics and photochemistry of single molecules and of molecular ensembles [10–12]. Recently, the possibility to control and exploit the angular momentum and the helicity of the cavity photons has received much attention [18–20]. Tuning the circular polarization of the polaritons can have profound implications in cavity-molecular processes [19,21], for instance, enantio-selectivity [20,22] and polariton ring currents [23]. This has lead to the design of various schemes that rely on the use of special mirrors and cavity configurations for controlling the polarization and helicity of cavity modes [19,20,24]. While the fundamental mechanisms of vibronic coupling involving molecules and a single cavity mode are well understood [4,10–13], vibronic interactions involving circular cavity-modes have, to the best of our knowledge, not been addressed so far. In highly symmetric molecular systems, degenerate electronic states become coupled via vibrational distortions of the molecular scaffold, which can be understood as an exchange of angular momentum between the electronic and vibrational subsystems [25]. Hence the natural question arises, to what extent do these vibronic effects extend to the otherwise noninteracting, circularly polarized cavity modes.

The symmetry point group of a molecule with an $n$-fold rotational axis $C_{n\geqslant 3}$ presents $(n-2)/2$ ($n$ even) or $(n-1)/2$ ($n$ odd) doubly degenerate irreducible representations associated with such an axis. One of these subspaces has degenerate electronic states that transform according to the $x$ and $y$ functions in real space, the two components being labeled $E_x$ and $E_y$ [26]. There are two properties of these $E$ electronic states that need to be considered: first, from simple selection rules, the two orthogonal polarization directions of light propagating parallel to the $C_n$ symmetry axis couple the totally symmetric $A$ ground electronic state of the molecules with the corresponding $E_{x/y}$ component of electronically excited states. Examples are found in the planar triazine or benzene molecules, featuring $C_3$ and $C_6$ rotation axes perpendicular to the molecular plane, respectively [26]. Second, inevitably, the presence of vibronic coupling between $E_x$ and $E_y$ states in the molecules caused by displacements along vibrational modes creates vibronic states with mixed electronic character, i.e., the well-known Jahn-Teller (JT) effect [25,27–30].

We consider now that molecules with these characteristics lie with their $C_n$ axes perpendicular to the mirrors of a Fabry-Perot (FP) cavity resonator (cf. Fig. 1). In this model, the molecules have no rotational degrees of freedom. They are assumed to be kept in their orientation through interaction with an environment, and we note that experiments in FP nanocavities take place in polymer matrices [18] or other condensed phases [31]. This configuration of the molecules and propagation direction of the FP electromagnetic modes results in the formation of JT polaritons, where the vibronically coupled electronic states of the molecules mix the two orthogonal polarization directions of the normal-incidence cavity modes. The theoretical description of the JT polaritonic states and their mixed polarization character is the main subject of our investigation. The effect of an external electromagnetic field on the dynamics of these states is described in the Supplemental Material (SM) [32].

Without loss of generality, we base our description of the mechanism of photonic-vibronic mixing of the two cavity polarization directions by considering the paradigmatic $(E\times e)$ JT Hamiltonian, where the $E$ electronic states are coupled by the doubly degenerate $e$ vibrational modes [25,27–29,33]. The $(E\times e)$ coupling mechanism occurs, for example, in molecules with a $C_3$ symmetry axis. The general properties of the $(E\times e)$ JT Hamiltonian have been well understood [25,27,28,34,35] in molecular spectroscopy as a

---

[*] krishna.nandipati@pci.uni-heidelberg.de

[†] oriol.vendrell@uni-heidelberg.de

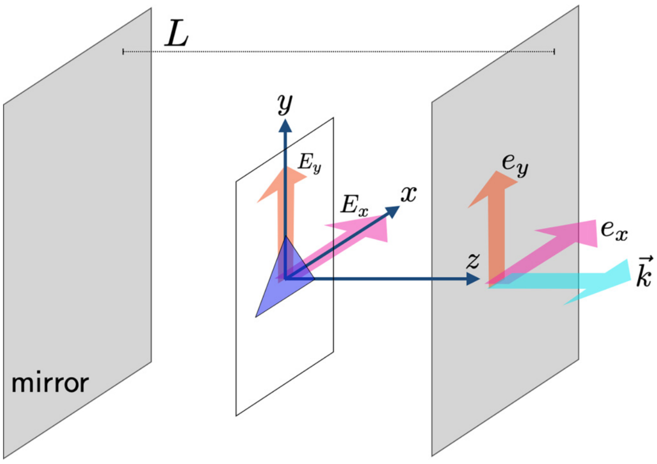

FIG. 1. Schematic of a JT active system situated inside the FP cavity. The symmetry axis of the JT system, represented by the triangular-shaped molecule, and the wave vector $\vec{k}$ of the $x(y)$-polarized cavity light point along the $z$ axis. The cavity is schematically represented by mirrors (in gray) separated by a distance $L$. The $x(y)$-polarized cavity mode interacts via dipole coupling with the $E_x(E_y)$ degenerate electronic excitation of the JT system.

premise to approach complex multimode vibronic interactions in polyatomic systems [29], thus making it an ideal model for investigating molecular nonadiabatic effects with cavity modes.

*Cavity Jahn-Teller Hamiltonian.* The cavity-JT (CJT) Hamiltonian is comprised of the JT molecular system plus the two normal-incidence modes of the FP cavity with polarization directions $(\vec{e}_x, \vec{e}_y)$, $\hat{H} = \hat{H}_{\rm JT} + \hat{H}_C + \hat{H}_{CM}$, where $\hat{H}_{\rm JT}$ is the linear $(E \times e)$ JT Hamiltonian, $\hat{H}_C$ is the cavity Hamiltonian, and $\hat{H}_{CM}$ is the light-matter coupling (see schematic in Fig. 1). $\hat{H}_{\rm JT}$ is represented in the diabatic basis of the excited $E$ electronic states $|E_{x(y)}(\boldsymbol{Q}_0)\rangle$, which are energetically well separated from the ground electronic state $|A(\boldsymbol{Q}_0)\rangle$. These electronic states are defined to be the eigenstates of $\hat{H}_{\rm JT} - \hat{T}_N$ (nuclear kinetic energy), the clamped-nuclei Hamiltonian, at the reference nuclear geometry $\boldsymbol{Q}_0$ [25]. For simplicity, in the following we drop the indication $\boldsymbol{Q}_0$ inside the diabatic electronic state *kets*.

In the electronic $\{|E_+\rangle, |A\rangle, |E_-\rangle\}$ basis, the molecular JT Hamiltonian reads

$$\hat{H}_{\rm JT} = \sum_{r=+,-} [\hbar\omega\, \hat{b}_r^\dagger \hat{b}_r\, \mathbf{1}_e + \epsilon(|E_r\rangle\langle E_r|)] + \frac{\kappa}{\sqrt{2}}\{(\hat{b}_+^\dagger + \hat{b}_-)|E_-\rangle\langle E_+| + \text{H.c.}\}, \qquad (1)$$

where $E_r$ refers to the complex electronic basis $|E_\pm\rangle = (|E_x\rangle \pm i|E_y\rangle)/\sqrt{2}$, $\mathbf{1}_e$ is the unit operator in the space of the electronic states, $\omega$, $\epsilon$, and $\kappa$ are the frequency of the $e$ modes, the energy of the $E$ electronic states at the reference geometry $\boldsymbol{Q}_0$, and the linear JT coupling parameter, respectively. The vibrational ladder operators are defined as $\hat{b}_\pm = (\hat{b}_x \mp i\hat{b}_y)/\sqrt{2}$ and $\hat{b}_\pm^\dagger = (\hat{b}_x^\dagger \pm i\hat{b}_y^\dagger)/\sqrt{2}$ [36]. Here $\hat{b}_x$ and $\hat{b}_y$ refer to ladder operators associated with the real and degenerate vibrational modes $Q_x$ and $Q_y$, respectively.

This representation of $\hat{H}_{\rm JT}$ makes particularly transparent that the vibronic coupling results in an exchange of angular momentum between the electronic subspace and the vibrational pseudorotation of the molecular scaffold, where the angular momentum perpendicular to the $(x, y)$ plane for the vibrational modes is given as

$$\hat{L}_z = \hbar(\hat{b}_+^\dagger \hat{b}_+ - \hat{b}_-^\dagger \hat{b}_-), \qquad (2)$$

where $\hat{b}_+^\dagger \hat{b}_+$ and $\hat{b}_-^\dagger \hat{b}_-$ are number operators for the vibrational modes with positive and negative angular momentum, respectively.

It will also be convenient to introduce an electronic angular-momentum-like operator within the $E$ subspace,

$$\hat{S}_z = \hbar(|E_+\rangle\langle E_+| - |E_-\rangle\langle E_-|), \qquad (3)$$

with eigenvalues $0, \pm\hbar$. The vibronic angular momentum of the molecular JT subsystem is defined as $\hat{J}_{\rm JT} = 2\hat{L}_z + \hat{S}_z$, where the factor 2 in front of $\hat{L}_z$ follows from the $\pi$-radians periodicity of the vibrational pseudorotation instead of $2\pi$ [28]. It is a simple exercise to check that $[\hat{H}_{\rm JT}, \hat{J}_{\rm JT}] = 0$, the well-known symmetry of the linear $(E \times e)$ JT Hamiltonian resulting in the double degeneracy of the vibronic spectrum. It is worth noting here that the spectrum of the *quadratic* JT Hamiltonian is also doubly degenerate due to the remaining symmetry, although $\hat{J}_{\rm JT}$ ceases to be a conserved quantity [28].

The coupling of each cavity polarization to the corresponding electronic excitation is now considered within the Condon approximation of constant transition dipole [37] and within the rotating wave approximation [36], where

$$\hat{H}_C = \hbar\omega_c(\hat{a}_+^\dagger \hat{a}_+ + \hat{a}_-^\dagger \hat{a}_-)$$
$$\hat{H}_{CM} = \frac{\Omega}{2}(\hat{a}_+^\dagger |A\rangle\langle E_+| + \hat{a}_-^\dagger |A\rangle\langle E_-| + \text{H.c.}). \qquad (4)$$

Here $\hbar\omega_c$ is the photon energy of the cavity modes, and $\Omega/2$ is the coupling strength between the molecule and the cavity modes in energy units. Hence, at zero detuning the Rabi splitting takes on the value $\Omega$ in units of energy. For the representation of $\hat{H}_C$ and analogously to Eqs. (1) and (2), we introduce circular cavity modes as linear combinations of the $(x, y)$ linear polarizations, $\hat{a}_\pm = (\hat{a}_x \mp i\hat{a}_y)/\sqrt{2}$ and $\hat{a}_\pm^\dagger = (\hat{a}_x^\dagger \pm i\hat{a}_y^\dagger)/\sqrt{2}$, where $\hat{a}_\pm^{(\dagger)}$ annihilate (create) cavity photons with $\pm\hbar$ angular momentum [36]. Here we should be reminded that the standing $(+/-)$–circular modes of a cavity with conventional mirrors have a nonzero angular momentum and thus a well-defined direction of rotation of the electric and magnetic fields in the plane of the cavity as seen by an external observer. However, they have no net helicity, which is defined as the projection of the angular momentum of a particle onto its linear momentum [18,19,38]. Thus, the helicities of the two counterpropagating photon modes that form the standing wave mutually cancel [38]. We refer to the circular cavity modes with either positive or negative angular momentum as cavity *polarizations*.

In the circular cavity-modes basis, the $z$ component of the photonic angular momentum of the FP cavity reads

$$\hat{l}_z = \hbar(\hat{a}_+^\dagger \hat{a}_+ - \hat{a}_-^\dagger \hat{a}_-). \qquad (5)$$

We note for clarity that up to this point we have introduced three partial angular momenta $\{L_z, l_z, S_z\}$ for the vibrational,

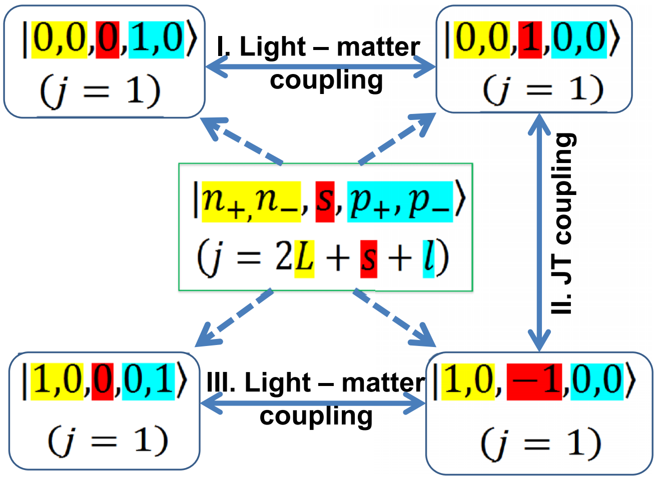

FIG. 2. Coupling of cavity modes (cyan) with (+) and (−) polarizations through molecular JT vibronic coupling (yellow): an initial one-photon state of (+) polarization of the cavity-JT system, $p_+ = 1$, transfers angular momentum to the $E_+$ electronic state of the molecule (red) through light-matter coupling (step I). The $E_+$ electronic state couples to $E_-$ by virtue of the JT coupling (step II), involving angular momentum exchange with the vibrations: the vibrational pseudorotation increases $n_+$ by one unit [see Eq. (1)]. The negative electronic angular momentum in the $E_-$ state finally couples to the cavity mode with (−) polarization via light-matter coupling, thus increasing $p_-$ by one (step III). Throughout the coupling mechanism, $j$ is conserved.

photonic, and electronic degrees of freedom, respectively, and caution the reader to not confuse $S_z$ with, e.g., a spin angular momentum, which is absent in the considered model. Defining the total vibronic-photonic angular momentum $\hat{J} = 2\hat{L}_z + \hat{S}_z + \hat{l}_z$ and using the JT commutation relation introduced above, one finds out that $\hat{J}$ is conserved for the CJT Hamiltonian (cf. SM [32]), $[\hat{H}, \hat{J}] = 0$. This commutation relation holds as well for molecular ensembles, where then $\hat{H} = \hat{H}_C + \sum_M (\hat{H}_{\mathrm{JT}}^{(M)} + \hat{H}_{CM}^{(M)})$ and $\hat{J}_{\mathrm{tot}} = \sum_M (2\hat{L}_z^{(M)} + \hat{S}_z^{(M)}) + \hat{l}_z$. Thus, the vibronic-photonic eigenstates of the CJT Hamiltonian can be cast as eigenstates of the total vibronic plus photonic angular momenta of the system and can be characterized by the quantum number $j = 2L + s + l$. Here $L$ is the angular momentum quantum number of the vibrational pseudorotation. In the circular modes basis, the vibrational angular momentum $L = n_+ - n_-$, where $n_\pm = 0, 1, \ldots$ are the number of left or right circular quanta, whereas $s = 0, \pm 1$ represents the electronic angular momentum quantum number associated with the $A$ and $E_\pm$ electronic states. $l = p_+ - p_-$, where $p_\pm = 0, 1$ is the total angular momentum quantum number of the circularly polarized cavity photons. The diagonalization of the cavity-JT Hamiltonian, Eqs. (1) and (4), yields the corresponding JT polaritonic eigenstates with mixed cavity polarization, referred to as the JT polaritons. The mechanism of $p_+$ and $p_-$ polarization mixing in the JT polaritons is illustrated in Fig. 2.

*Polarization properties of the JT polaritons.* The expectation value of the angular momentum of the cavity photons in the JT polaritonic state $|k_j\rangle$ is given by $\mathcal{P}_k^{(j)} = \langle k_j|\hat{l}_z|k_j\rangle$ where, by symmetry, $\mathcal{P}_k^{(1)} = -\mathcal{P}_k^{(-1)}$. We illustrate the

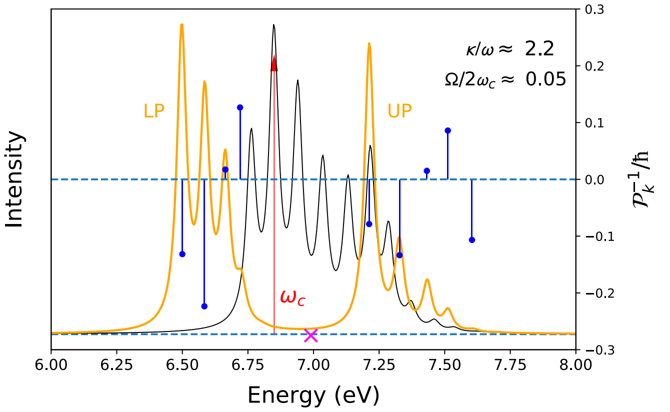

FIG. 3. The absorption spectrum of the $(E \times e)$ JT model of sym-triazine (in black) and the spectrum of the same system coupled to the FP cavity (in orange) in Fig. 1. Absorption lines are convoluted with a 44-meV Lorentzian shape. The spectrum corresponds to the absorption by RCP light propagating along the $z$ axis from right to left according to the schematic in Fig. 1. The $\omega_c$ is set at the energy of the most optically bright state of the bare JT spectrum (indicated with red arrow) of the triazine, which is lying below the CI energy $\epsilon$ (marked × on the energy axis). The expectation value of the photon polarization for each JT polaritonic eigenstate $\mathcal{P}_k^{-1}/\hbar$ is shown in blue (middle $y$ axis).

dependency of the cavity polarization on model with parameters $\omega = 0.003$ a.u. ($\approx 660\,\mathrm{cm}^{-1}$) and $\epsilon = 7$ eV [cf. Eq. (1)], which are in the typical range for JT active vibrational modes and vertical electronic transitions of organic molecules such as benzene ($D_{6h}$) [39] and sym-triazine ($D_{3h}$) [30].

Figure 3 presents the JT polaritonic spectrum of the CJT model of sym-triazine with the JT coupling, $\kappa/\omega = 2.2$ [30] and the cavity coupling, $\Omega/2\omega_c = 0.05$. The states in the CJT system are doubly degenerate, characterized by $j = \pm 1$, and we show the spectrum of the $j = -1$ block, which is reached from the overall ground state through absorption of right-circularly polarized (RCP) light propagating from right to left along the $z$ direction when comparing with the schematic in Fig. 1. The response of the cavity polarization to external circularly polarized light pulses is discussed in the SM [32]. The spectrum splits into lower polariton (LP) and upper polariton (UP) branches that are separated by $\Omega$, and it shows the net polarization $\mathcal{P}_k$ (in $\hbar$ units) of the $j = -1$ block eigenstates with blue lines. The JT polaritonic states feature different amounts of photon polarization, which, however, are in absolute value about an order of magnitude below the theoretical maximum of $\pm\hbar$.

This point is clearly seen by inspecting the photon polarization $\mathcal{P}_k$ for the most optically bright $k_{-1}$ state as a function of cavity-molecule coupling ($\Omega/2\omega_c$) in Fig. 4 for selected JT couplings ($\kappa/\omega$), where the major cause of polarization mixing is the molecular JT coupling. The polarization of the JT polaritonic states as a function of $\Omega/2\omega_c$ can be suppressed by up to one order of magnitude compared to $-\hbar$ at the vibronic coupling corresponding to the triazine molecule (purple curve). This suppression starts even for weak cavity-molecule couplings for a given JT coupling. At $\kappa/\omega = 0$, the light and matter (pure electronic excitation in this case)

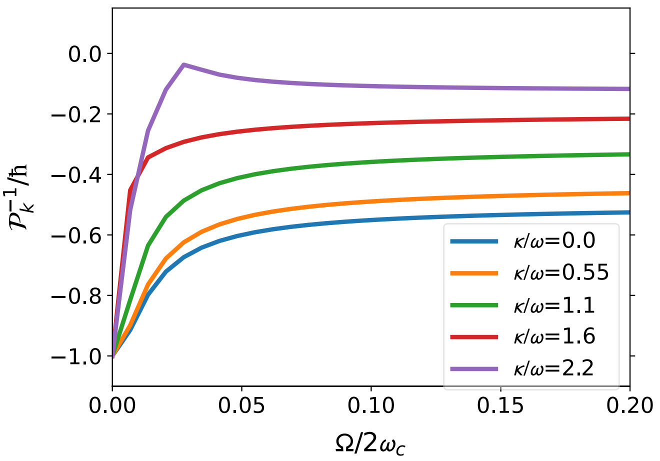

FIG. 4. Expectation value of the cavity polarization for the most optically bright $k$ state within $j = -1$ block as a function of the cavity-molecule couplings ($\Omega/2\omega_c$) at selected JT coupling ($\kappa/\omega$).

nonetheless hybridize, and the absolute value of the polarization correspondingly reduces from 1 to at most 0.5. The effect of the JT coupling further reduces the maximum polarization of the JT polaritonic states by admixing the two polarization directions through the mechanism described around Fig. 2.

Importantly, some of the states in the spectrum of Fig. 3 feature the opposite polarization direction (in this case positive mean polarization $\mathcal{P}_k$) compared to the polarization of an uncoupled cavity state reached by RCP light (which is $-\hbar$). This occurs despite that all JT-polaritonic states belong to the $j = -1$ block. Therefore these states are reached exclusively through excitation by external RCP light (LCP for $j = 1$ correspondingly), see SM [32]. We refer to these JT polariton states as *inverse polarization* states. Two remarks are in order here. (i) This effect is entirely due to the photonic-vibronic coupling. By removing the second line in Eq. (1) the exchange of angular momentum between the cavity modes and the molecule ceases to operate, and no polarization mixing is possible. (ii) The existence of JT polaritonic *eigenstates* with a finite polarization $\mathcal{P}_k^{(j)}$ requires necessarily the existence of a degenerate electronic subspace in the molecule such that complex eigenstates with angular momentum (i.e., stationary electronic currents) exist [40].

*Conclusions.* A JT system (or an aligned ensemble thereof) couples to the two polarization directions (photonic angular momenta) of the normal-incidence modes of a FP resonator by virtue of the molecular vibronic coupling. The JT polaritonic states have a mixed contribution of the two cavity polarizations, which is inherited from their mixed electronic-excitation character. Two main effects are observed: on the one hand a much reduced net polarization compared to the uncoupled vibronic-photonic case ($\kappa \to 0$ limit, or alternatively, fixed nuclei in space), and on the other hand the presence of inverted polarization states. A key consequence of the latter is that the net polarization of the hybrid cavity-matter system becomes energy dependent (cf. Fig. 3). Hence external pulses of the same circular polarization but with different frequency components can generate different polarization responses of the system [32]. This realization can have important consequences for the development of spectroscopic techniques in cavity environments using circularly polarized light and can result in schemes to achieve chiral environments in cavities without resorting to special types of mirrors [18]. The existence of JT-polaritonic states with inverted polarization could be verified by pump-probe spectroscopic measurements of JT systems embedded in FP nanocavities and using circularly polarized pulses [41,42].

*Acknowledgments.* This work has been supported by the collaborative research center “SFB 1249: N-Heteropolyzyklen als Funktionsmaterialen” of the German Research Foundation (DFG). We thank Prof. Wolfgang Domcke for useful comments on the manuscript.

---

[1] J. A. Hutchison, T. Schwartz, C. Genet, E. Devaux, and T. W. Ebbesen, Angew. Chem. Int. Ed. **51**, 1592 (2012).

[2] T. Schwartz, J. A. Hutchison, J. Léonard, C. Genet, S. Haacke, and T. W. Ebbesen, Chem. Phys. Chem. **14**, 125 (2013).

[3] F. Herrera and J. Owrutsky, J. Chem. Phys. **152**, 100902 (2020).

[4] R. F. Ribeiro, L. A. Martínez-Martínez, M. Du, J. Campos-Gonzalez-Angulo, and J. Yuen-Zhou, Chem. Sci. **9**, 6325 (2018).

[5] M. Kowalewski, K. Bennett, and S. Mukamel, J. Chem. Phys. **144**, 054309 (2016).

[6] J. Galego, F. J. Garcia-Vidal, and J. Feist, Nat. Commun. **7**, 13841 (2016).

[7] J. Flick, M. Ruggenthaler, H. Appel, and A. Rubio, Proc. Natl. Acad. Sci. USA **114**, 3026 (2017).

[8] J. Feist, J. Galego, and F. J. Garcia-Vidal, ACS Photonics **5**, 205 (2018).

[9] O. Vendrell, Chem. Phys. **509**, 55 (2018).

[10] F. Herrera and F. C. Spano, Phys. Rev. Lett. **116**, 238301 (2016).

[11] F. Herrera and F. C. Spano, Phys. Rev. Lett. **118**, 223601 (2017).

[12] O. Vendrell, Phys. Rev. Lett. **121**, 253001 (2018).

[13] A. D. Dunkelberger, B. S. Simpkins, I. Vurgaftman, and J. C. Owrutsky, Annu. Rev. Phys. Chem. **73**, 429(2022).

[14] G. Morigi, P. W. H. Pinkse, M. Kowalewski, and R. de Vivie-Riedle, Phys. Rev. Lett. **99**, 073001 (2007).

[15] T. W. Ebbesen, Acc. Chem. Res. **49**, 2403 (2016).

[16] E. Orgiu, J. George, J. Hutchison, E. Devaux, J. Dayen, B. Doudin, F. Stellacci, C. Genet, J. Schachenmayer, C. Genes *et al.*, Nat. Mater. **14**, 1123 (2015).

[17] X. Wang, E. Ronca, and M. A. Sentef, Phys. Rev. B **99**, 235156 (2019).

[18] J. Gautier, M. Li, T. W. Ebbesen, and C. Genet, ACS Photonics **9**, 778 (2022).

[19] H. Hübener, U. De Giovannini, C. Schäfer, J. Andberger, M. Ruggenthaler, J. Faist, and A. Rubio, Nat. Mater. **20**, 438 (2021).

[20] J. Feis, D. Beutel, J. Köpfler, X. Garcia-Santiago, C. Rockstuhl, M. Wegener, and I. Fernandez-Corbaton, Phys. Rev. Lett. **124**, 033201 (2020).

[21] I. A. Shelykh, A. V. Kavokin, Y. G. Rubo, T. Liew, and G. Malpuech, Semicond. Sci. Technol. **25**, 013001 (2010).

[22] S. J. Yoo and Q.-H. Park, Phys. Rev. Lett. **114**, 203003 (2015).

[23] S. Sun, B. Gu, and S. Mukamel, Chem. Sci. **13**, 1037 (2022).

[24] B. Abasahl, S. Dutta-Gupta, C. Santschi, and O. J. Martin, Nano Lett. **13**, 4575 (2013).

[25] I. B. Bersuker, *The Jahn-Teller Effect* (Cambridge University Press, Cambridge, England, 2006).

[26] D. C. Harris and M. D. Bertolucci, *Symmetry and Spectroscopy: An Introduction to Vibrational and Electronic Spectroscopy*, new edition (Dover Publications, New York, 1989).

[27] R. Englman, *The Jahn–Teller Effect in Molecules and Crystals* (Wiley, New York, 1972).

[28] H. C. Longuet-Higgins, U. Öpik, M. H. L. Pryce, and R. A. Sack, Proc. R. Soc. A **244**, 1 (1958).

[29] H. Köppel, W. Domcke, and L. Cederbaum, Adv. Chem. Phys. **57**, 59 (1984).

[30] R. L. Whetten, K. S. Haber, and E. R. Grant, J. Chem. Phys. **84**, 1270 (1986).

[31] F. Schlawin, D. M. Kennes, and M. A. Sentef, Appl. Phys. Rev. **9**, 011312 (2022).

[32] See Supplemental Material at http://link.aps.org/supplemental/10.1103/PhysRevA.107.L061101 for the derivation of the commutation relation $[\hat{H}, \hat{J}] = 0$ and the discussion of the polarization dynamics of Jahn-Teller polaritons triggered by circularly polarized pulses. It also provides technical details about the quantum dynamical simulations.

[33] H. A. Jahn and E. Teller, Proc. R. Soc. A **161**, 220 (1937).

[34] W. Moffitt and A. Liehr, Phys. Rev. **106**, 1195 (1957).

[35] M. D. Sturge, Solid State Phys. **20**, 91 (1968).

[36] M. D. Crisp, Phys. Rev. A **43**, 2430 (1991).

[37] D. J. Tannor, *Introduction to Quantum Mechanics: A Time-Dependent Perspective* (University Science Books, Melville, NY, 2007).

[38] S. M. Barnett, R. P. Cameron, and A. M. Yao, Phys. Rev. A **86**, 013845 (2012).

[39] G. A. Worth, J. Photochem. Photobiol. A **190**, 190 (2007).

[40] K. R. Nandipati and O. Vendrell, Phys. Rev. Res. **3**, L042003 (2021).

[41] V. Svoboda, M. D. Waters, D. Zindel, and H. J. Wörner, Opt. Express **30**, 14358 (2022).

[42] D. Baykusheva, M. S. Ahsan, N. Lin, and H. J. Wörner, Phys. Rev. Lett. **116**, 123001 (2016).